# We are IntechOpen, the world's leading publisher of Open Access books Built by scientists, for scientists

6,900
Open access books available

185,000
International authors and editors

200M
Downloads

Our authors are among the

154
Countries delivered to

TOP 1%
most cited scientists

12.2%
Contributors from top 500 universities




WEB OF SCIENCE™

Selection of our books indexed in the Book Citation Index in Web of Science™ Core Collection (BKCI)

## Interested in publishing with us?
## Contact book.department@intechopen.com

Numbers displayed above are based on latest data collected.
For more information visit www.intechopen.com



# 11

# Radionuclide and Contaminant Immobilization in the Fluidized Bed Steam Reforming Waste Product

James J. Neeway[1], Nikolla P. Qafoku[1], Joseph H. Westsik Jr.[1], Christopher F. Brown[1], Carol M. Jantzen[2] and Eric M. Pierce[3]
[1]*Pacific Northwest National Laboratory, Richland, WA,*
[2]*Savannah River National Laboratory, Aiken, SC,*
[3]*Oak Ridge National Laboratory, Oak Ridge, TN,*
*USA*

## 1. Introduction

The goal of this chapter is to introduce the reader to the Fluidized Bed Steam Reforming (FBSR) process and resulting waste form. The first section of the chapter gives an overview of the potential need for FBSR processing in nuclear waste remediation followed by an overview of the engineering involved in the process itself. This is followed by a description of waste form production at a chemical level followed by a section describing different process streams that have undergone the FBSR process. The third section describes the resulting mineral product in terms of phases that are present and the ability of the waste form to encapsulate hazardous and radioactive wastes from several sources. Following this description is a presentation of the physical properties of the granular and monolith waste form product including and contaminant release mechanisms. The last section gives a brief summary of this chapter and includes an overview of strengths associated with this waste form and needs for additional data. The reader is directed elsewhere for more information on other waste forms such as Cast Stone (Lockrem, 2005), Ceramicrete (Singh et al., 1997, Wagh et al., 1999) and geopolymers (Kyritsis et al., 2009; Russell et al., 2006).

Classical steam reforming is a versatile process that decomposes organic materials through reactions with steam (Olson et al., 2004a). Steam reforming has been used on a large scale by the petrochemical industry to produce hydrogen for at least 65 years. If the material being reformed contains halogens, phosphorus, or sulfur, mineral acids are also formed (e.g., hydrochloric acid, phosphorous acid, phosphoric acid, and hydrogen sulfide) unless inorganic materials capable of scavenging these species are present in the waste or additives (Nimlos & Milne, 1992; Olson et al., 2004a). Organic nitrogen is converted to $N_2$, and organic oxygen is converted to CO or $CO_2$ (Olson et al., 2004a). In the presence of a reducing agent such as organic carbon, nitrates and nitrites are converted to nitrogen gas (Vora et al., 2009). The waste feed may be either basic or acidic (Lorier et al., 2005). Alkali elements, including sodium, potassium, and cesium in the wastes, "alkali activate" the unstable $Al^{3+}$ in the clay to form new mineral phases. The other waste component cations and anions are captured in the cage structures of the sodium aluminosilicate minerals.

In 1999, the Studsvik facility in Erwin, Tennessee demonstrated the ability to commercialize the FBSR process (Mason et al., 2003). The facility uses steam reforming based on a process known as THermal Organic Reduction (THOR®). The THOR® FBSR process is being used commercially to process liquid radioactive waste waste streams, including ion exchange resins, charcoal, graphite, sludge, oil, and solvents that contain up to ~4.5 $\times 10^5$ Sv/hr (Mason et al., 2003). Steam reforming thermally treats wastes at temperatures ranging from 625 to 750°C using a fluidized bed reformer (Vora et al., 2009). During mineralization with superheated steam, organic matter is converted to carbon dioxide and steam, while nitrates and nitrites are reduced to nitrogen. The non-volatile solids in the residue are converted to water-insoluble stable crystalline minerals that incorporate contaminants.

Other THOR Treatment Technologies, LLC (TTT) designed FBSR testing platforms have also been built and used to demonstrate steam reforming technologies for the immobilization of radioactive and simulant wastes at the bench-, pilot-, and engineering-scale. An FBSR facility is being designed and constructed at Idaho National Engineering and Environmental Laboratory (INEEL) for the treatment of sodium-bearing waste (SBW) to be sent for disposal at the Waste Isolation Pilot Plant (WIPP) in Carlsbad, New Mexico (Marshall et al., 2003; Olson et al., 2004b; Soelberg et al., 2004a). Another such facility is being considered for converting Savannah River Site (SRS) salt supernate waste (Tank 48), containing nitrates, nitrites, and cesium tetraphenyl borate (CsTPB) to carbonate or silicate minerals which are compatible with subsequent vitrification (Soelberg et al., 2004b). Pilot-scale testing has also been performed for other DOE wastes including Waste Treatment Plant-Secondary Waste (WTP-SW) and Hanford Low-Activity Waste (LAW).

Another system called the Bench-Scale Reformer (BSR) has been developed at Savannah River National Laboratory (SRNL) to help assess the suitability and effectiveness of the FBSR process for the treatment of Hanford LAW (Burkett et al., 2008). The major difference between the FBSR and BSR designs is that the BSR bed is not completely fluidized due to its containment in shielded cells, restricting the height necessary to allow for this process disengagement (Burket et al., 2008). Mineralization is still created by the BSR steam reforming reactions and homogenization occurs by turbulent mixing after sample formation.

### 1.1 Fluidized bed steam reformer process description

A typical THOR® mineralizing FBSR process can use either a single reformer or dual reformer. The dual reformer flowsheet is only needed if the waste being mineralized contains organics that need to be destroyed. Currently, there is no flowsheet for encapsulating the FBSR granular product in a binder to produce a monolithic waste form although this has been proven at the bench-scale. The dual reformer consists of the following primary subsystems (Olson et al., 2004b):

1. A feed for gases, liquids, slurries, and co-additives such as clay and denitration catalysts;
2. The fluidized bed reactor vessel known as the Denitration and Mineralization Reformer (DMR)
3. A high temperature filter (HTF) to catch fines and recycle them to the DMR bed to act as seeds for particle size growth;
4. The solid and product collection from the DMR and HTF;
5. The off-gas treatment which can include the second reformer known as the Carbon Reduction Reformer (CRR);
6. The monitoring and control of the system.

The FBSR process used for mineralizing high sodium wastes (nitrate and/or hydroxide) can use either a single reformer flowsheet, the denitration DMR, or a dual reformer flowsheet, including a CRR, to handle organics, as shown in Figure 1.

The DMR operating temperature is maintained at 700 to 750°C for generating the sodium aluminosilicate (Na-Al-Si or NAS) end product. The flow diagram shows the feed preparation, denitration and mineralizing, and off-gas portions of the FBSR process. All mineralization reactions take place in the DMR. Granular products are removed from the bottom of the DMR and finer product solids are separated from the process outlet gases by the HTF. The finer HTF mineral solids can be recycled back to the DMR bed as seed material to the DMR bed, as shown in Figure 1, or the HTF mineral solids can be combined with the granular mineral solids from the DMR to make a monolith. The process outlet gases are treated in the off-gas treatment system to meet air permit emission limits. In the application of FBSR to Hanford wastes, a clay mineralizing agent, any reductants, and any catalysts are co-added to the DMR along with the waste(s) in the feed tank as shown in Figure 1. The bed is fluidized with superheated steam and near-ambient pressure. A carbon source, such as coal, wood product, or sucrose, is injected into the bed as a fuel source and reducing/denitration agent. Within the fluidized bed, the waste-feed droplets coat the bed particles and rapidly dry. Nitrates, nitrites, and organics are destroyed (TTT, 2009; Vora et al., 2009). In the steam environment, the clay mineralizing agent injected with the wastes becomes unstable as hydroxyl groups are driven out of the clay structure (Jantzen, 2008). The clays become amorphous, and the silicon and aluminum atoms become very reactive.

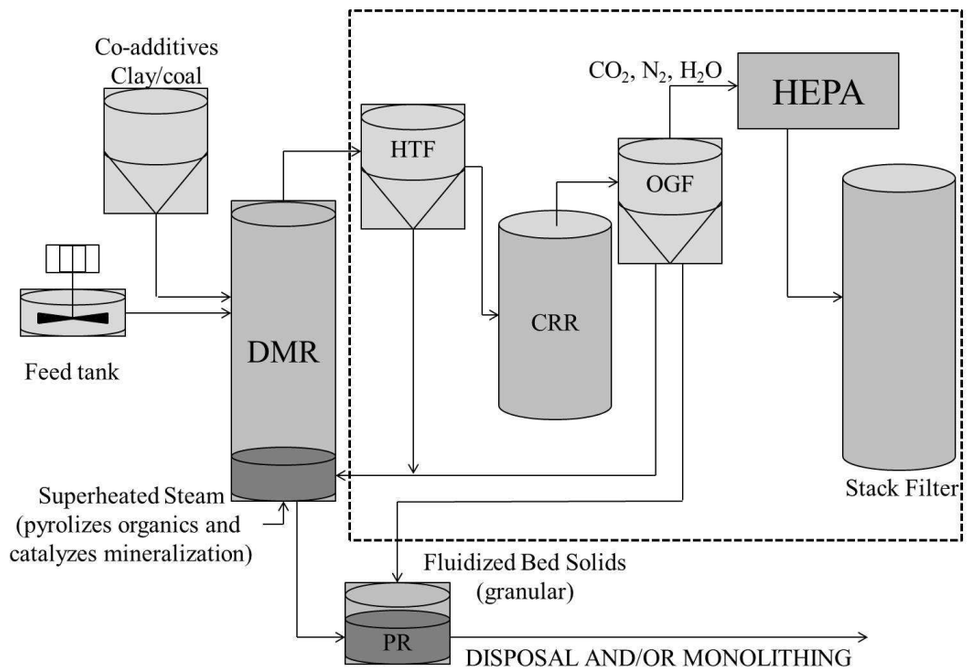



Fig. 1. FBSR Sodium Aluminosilicate (NAS) Waste Form Dual Processing Flowsheet
(DMR = Denitration & Mineralizing Reformer; PR = Product Receiver;
HTF = High Temperature Filter (material recycled to DMR); CRR = Carbon Reduction Reformer (treats gases only); OGF = Off-Gas Filter; HEPA = High-Efficiency Particulate Air filter) (Adapted from Jantzen, 2008)

### 1.1.1 Denitration and Mineralization Reformer

The DMR is a fluidized bed reformer with the bed media being fluidized using superheated steam injected by a distributor at the bottom of the vessel. Granular carbon is also fed directly into the bed to provide energy for the process. The reaction of solid carbon with steam generates carbon monoxide and hydrogen, via the water/gas reaction (see Olson et al., 2004b for a list of reactions). A small amount of oxygen is bled in to react with any excess hydrogen to create more steam and heat because the reaction of oxygen and hydrogen is exothermic. A metered flow of atomizing compressed air is used to atomize the waste/clay slurry introduced to the bed. As the waste/clay slurry is injected into the bed by the waste feed injectors, mineral products are formed by the hydrothermal reaction of the alkali metals (sodium, cesium, and potassium) with the added clay (aluminosilicate). The reaction may also involve clay and alkaline earths or other inorganics in the waste. DMR bed materials consist of accumulated mineral stable, leach-resistant product granules that are fluidized by the low-pressure steam.

When the waste feed is introduced into the fluidized bed as fine spray, the waste feed reacts to form new minerals after contacting the heated fluidized bed. Nitrates and nitrites in the feed react with reductive gases to produce mainly nitrogen gas with traces of $NO_x$. The non-volatile contaminant constituents, such as metals and radionuclides, are mineralized by being incorporated into the final mineral species in the bed product. The process gases exit the DMR through the HTF and consist mainly of steam, $N_2$, CO, $CO_2$, and $H_2$. Some low levels of $NO_X$, acid gases, and short-chained organics may also be present and these can be destroyed in the CRR.

### 1.1.2 Off-gas treatment system

The off-gas treatment system provides high-efficiency filtration and oxidation of any residual volatile organics and small amounts of carbon monoxide and hydrogen from the DMR. The process off-gas from the DMR is routed into a HTF to trap small mineral product particles called fines. The gases pass through the carbon reduction reformer (CRR) to reduce residual $NO_X$ to $N_2$ in the lower reducing zone and to oxidize CO, $H_2$, and the residual hydrocarbons into $CO_2$ and water vapor in the upper oxidizing stage of the CRR. The CRR has a semi-permanent bed media composed of alumina. No additional $NO_X$ abatement or acid gas removal is required because the nitrates and nitrites are converted into nitrogen gas inside the DMR and CRR with a very high efficiency (TTT, 2009). Acid gases are minimized as the S, Cl, and F are incorporated into the bed product mineral structures such that no wet scrubber is required to remove acid gases in the off-gas treatment system. The off-gas from the CRR is cooled and then passes a through a Off-Gas Filter (OGF) and then through a high-efficiency particulate air (HEPA) filter to remove any further particulates. Further cooling occurs in an off-gas cooler and the off-gas is then passed through another set of HEPA filters and a mercury adsorber (if needed) before being exhausted out of a stack. The FBSR process outlet gases are compliant with Maximum Achievable Control Technology (MACT) limits for metals, $HCl/Cl_2$, particulates, dioxins/furans, volatile and semi-volatile organic compounds, total hydrocarbon, and carbon monoxide as well as site discharge limits for $NO_X$ and $SO_X$ (TTT, 2009; Vora et al., 2009).

### 1.2 Process control

Waste form process monitoring and control are necessary to obtain the desired mineral product. The proper amount of additives and operation in the proper REDuction/OXidation (REDOX) range ensure autocatalytic heating and pyrolysis. Mineralization control produces the desired NAS phases and is based on the MINCALC™ process control system (See Section 2.1.1). This strategy favors the formation of nepheline and sodalite.

To assist in finding the process REDOX potentials, an Electromotive Force (EMF) series developed by Schreiber (2007) is used to determine what the oxygen fugacity in the DMR is during mineralization. Iron, in the form of $Fe^{3+}(NO_3)$ is added as a REDOX indicator and the final product REDOX is measured spectrochemically using the Baumann method (Baumann, 1992). By measuring the ratio of $Fe^{+2}/\Sigma Fe$ in the resulting mineral product, the EMF is used to back calculate the oxidation of the remaining multivalent species of interest, e.g. S, Re, Cr. This calculation is more accurate if the unreacted coal in the bed product is less than 10 wt%. All control boundaries lead to a complete denitration of the product. Typically the FBSR process is run with a reducing environment with a log oxygen fugacity of -15 to -16 Pa.

## 2. FBSR waste form process description

Kaolin clay, the aqueous waste stream, steam, and a carbon or other heat source, are the only ingredients for the FBSR NAS granular product. This mix of liquids, solids, and gases is provided through feed subsystems in order to obtain a desired FBSR process material and conditions. The granular product is removed from the FBSR either as product from the bottom of the bed or as particulates removed from the fluidizing gases by the HTF. Unless the HTF particulates are recycled to the DMR bed as seed particles, these two materials are then combined and encapsulated in a binder for final disposal. This section gives a more detailed description of the additives used in the FBSR process.

### 2.1 Waste form ingredients

#### 2.1.1 Kaolin clay

Kaolin clay is a key ingredient in the FBSR process. In kaolin clay, the aluminum atom is octahedrally coordinated with bonds to two oxygen atoms and four hydroxyl ions. During processing at 700-750°C, the kaolin clay is destabilized and the four OH- atoms are vaporized which leaves the clay Al atoms unstable and amorphous at the nanoscale. Alkalis in the waste react with the unstable Al atom and rearrange to form a crystalline mineral species with a low free energy tetrahedral configuration such as $NaAlSiO_4$.

Several sources of kaolin clay have been used in the FBSR pilot-scale testing program with Table 1 listing some of their properties. SnoBrite and OptiKasT kaolin clays were used for tests with Hanford LAW (Olson et al., 2004b) while Troy and K-T Sagger XX kaolin clays were used for tests with INEEL SBW (Olson et al., 2004a). All of these kaolin clays were investigated for use as a mineralizing additive in the INEEL pilot-scale experiments. All the clays were evaluated based on XRD, particle-size analyses, whole element chemistry, and rheological properties (Olson et al., 2004b).

| Clay | Major Phases | Minor phases | Si:Al atom ratio | Total moisture (wt %) | Particle size (wt% less than 10% - 50% - 90%) | Particle density (g/cm3) |
|---|---|---|---|---|---|---|
| SnoBrite | Kaolinite[a] | Muscovite[b]; Rutile ($TiO_2$) possible | 1.02 | 14.20% | 0.82µm – 5.00µm – 20.8µm | 2.77 |
| OptiKasT | Kaolinite[a] | Muscovite [b] | 1.04 | 15.15% | 0.74µm – 4.22µm – 15.9µm | 2.69 |
| Troy | Kaolinite[a] | Muscovite [c]; Quartz ($SiO_2$) possible | 01:01.2 | 14.65% | 1.83µm – 14.83µm – 57.1µm | 2.74 |
| K-T Sagger XX | Kaolinite[d] | Muscovite[b] Rutile ($TiO_2$) | 01:01.7 | 10.60% | 1.34µm – 6.55µm – 21.5µm | 2.73 |

(a) Kaolinite (PDF#75-1593) ($Al_2O_3 \cdot 2SiO_2 \cdot 2H_2O$)
(b) Muscovite (PDF#07-0042) $(K, Na)(Al, Mg, Fe)_2\text{-}(Si_{3.1}Al_{0.9})O_{10}(OH)_2$
(c) Muscovite (PDF#86-1385) $((K_{0.86}Al_{1.94})(Al_{0.965}Si_{2.895}O_{10})\text{-}((OH)_{1.744}F_{0.256})$
(d) Kaolinite (PDF#78-1996)

Table 1. Properties of Kaolin Clays Used in FBSR Pilot Scale Tests (from Olson et al., 2004b, 2004b)

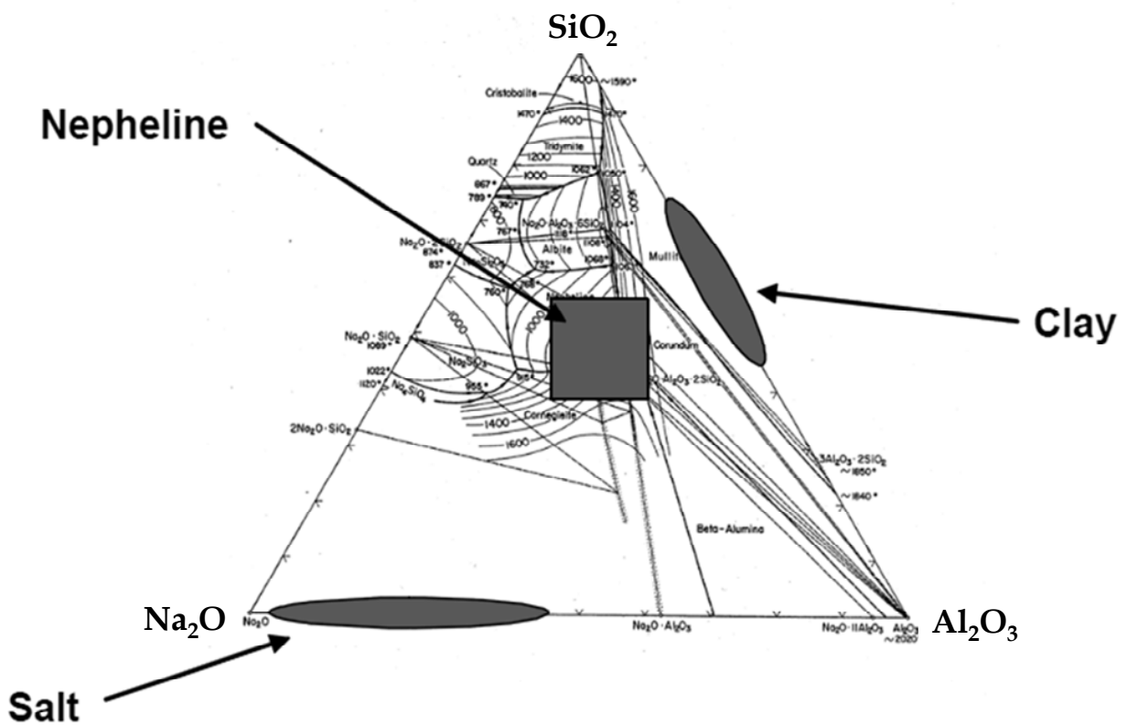



Fig. 2. Ternary Diagram Showing Guidelines for Kaolin Clay Selection (from Crawford & Jantzen, 2007)

The mineralizing agent needs to have a Si/Al that will react with the liquid waste and produce desired minerals. The kaolin clay type was selected with the appropriate Al:Si mole ratio that would suitably react with the Na and anions in the waste liquids. Usually, a ternary phase diagram (such as the one depicted in Figure 2) shows the target region of compositions that is thought to be the most favorable for producing the desired mineral products (Crawford & Jantzen, 2007). Similar diagrams may be seen in Olson et al. (2004a) and TTT (2009) for Hanford LAW and WTP-SW wastes, respectively. The most favorable atomic ratios that would produce the desired nepheline and sodalite products are thought to be $1 < M/Si < 1.33$, $1 < M/Al < 1.33$, $1 \leq Al/Si$, and $M/(Al+Si) = 0.5\text{-}0.67$, where M represents an alkali metal, mostly Na in this case. Atomic ratios provide guidelines due to the possibility of significant substitution of different alkali and alkaline earths, and some Fe for Al, in these feldspathoid minerals (Olson et al.c 2004a). SRNL has developed a spreadsheet called MINCALC™ that can be used as a tool to select the clay formulation and carbon addition and to make adjustments, such as accounting for extra aluminum and potassium in the wastes (Crawford & Jantzen, 2007; Pareizs et al., 2005). Additional considerations for choosing the optimum mineralizing additive include particle-size distribution that is optimized to make sure that as much clay as possible reacts with the liquid waste as well as eliminating clays that contain additional elements that will not react to form the desired mineral phases.

### 2.1.2 Carbon source

Different reductants (e.g., charcoal, carbon, or sugar) are used in the FBSR process to aid in pyrolyzing organics, and removing nitrate. Charcoal or carbon plus steam creates $H_2$ for autocatalytic heating, while sugar is not a good heat source and can only be used for the denitration and pyrolysis. For example, different types of carbon were considered to be used as reductants in the INEEL pilot-scale experiment (Olson et al., 2004a, 2004b). Carbon was evaluated based on reactivity, particle size, particle fracturing (attrition) resistance, moisture content, loss on ignition, and the ash composition. A wood-based carbon was chosen based on its efficient performance

### 2.1.3 Other properties of the starting bed

The primary solid feed material in the fluidized bed reactor consists of granular carbon and an initial starting bed media. The chosen starting material must be dense, inert, and have a high heat capacity due to high processing temperatures (Olson et al., 2004b). Bed materials that meet these criteria that were considered for an INEEL pilot-scale steam reformer were alumina, dolomite, sintered bauxite beads, nepheline syenite, and sintered calcium silicate (Olson et al., 2004b). Choice of starting bed material was based on composition, melting point, resistance and durability, particle size, and availability of the material. 70-grit alumina was finally chosen for the test. Alumina facilitates processing through its high heat capacity which transfers heat to the atomized feed and prevents over-quenching in the feed zone. Also, hot alumina does not seem to be coated by the product and was chosen because of its attrition resistance and inertness (Olson et al., 2004a). The 2008 Hanford LAW and WTP-SW pilot-scale tests at the Hazen Research Inc. (HRI) facility also used alumina as the starting bed material.

### 2.2 Process details

After startup, the FBSR process is straightforward. The feeds for the clay and tank wastes are fed into the FBSR. Products exiting through the DMR are passed through the HTF or recycled back into the DMR. The granular product is collected and allowed to cool before sending to the binder station for encapsulation into a monolith.

A last step in FBSR, as related to radioactive waste management, is the product must be encapsulated to meet disposal system requirements for compressive strength and to minimize the dispersability of the material. Several binders have been tested (Jantzen, 2006; TTT, 2009) and further testing and development is anticipated before a final form is selected. Simple, inexpensive binders, such as a cementitious material, a geopolymer, or Ceramicrete, are likely candidates. The geopolymer appears to be the most promising.

### 2.3 FBSR process chemistry

Two major processes occur simultaneously in the steam reforming of a nitrate salt: the mineralization process and the denitration process. Mineralization is the reaction of activated clay with estranged cations (Na, Cs, Tc, etc.) and other species present in the salt waste (Cl, F, I, $SO_4$, etc.). Stable crystalline clays become reactive amorphous clays at FBSR processing temperatures because clays lose their hydroxyl groups above 550°C. The waste species react with the reactive amorphous meta-kaolin-clay to form new stable crystalline mineral structures allowing formation and templating of mineral structures at moderate temperatures. The resulting stable crystalline structures leave the process as a granular solid product. Iron-bearing co-reactants can be added during processing to stabilize multivalent hazardous species present in the waste in durable spinel phases, i.e. Cr, Ni, Pb iron oxide minerals. Denitration, in the presence of a carbon source, is the reformation of the $NO_3$ and $NO_2$ anions to $N_2$, $H_2O$ (steam) and $CO_2$.

## 3. FBSR waste form description

The FBSR waste form is composed of two main components: a granular product and an encapsulating binder material. The primary granular product made by processing wastes in the FBSR is formed of geophases (minerals). These phases may provide leach resistant (durable) waste forms for immobilizing the contaminants that are present in different waste liquids (Olson et al., 2004a). This granular product is then encapsulated in a binder material to form a monolith which limits dispersability and provides some structural integrity for subsidence prevention in the disposal facility. The existing FBSR waste form data are derived from a number of pilot-scale FBSR tests conducted with INEEL SBW and Hanford LAW and secondary waste simulants. Table 2 summarizes these tests.

### 3.1 Sodium aluminosilicate (NAS) primary waste form

#### 3.1.1 Major mineral form attributes

The primary product from the FBSR process with kaolin clay is a granular product composed of NAS minerals which bond with radionuclides and contaminants of concern (COCs). The NAS FBSR granular product is a multiphase mineral assemblage of NAS feldspathoid group minerals (sodalites, nosean, and nepheline) with cage and ring

structures that sequester anions and cations (Jantzen et al., 2007). The nomenclature of this series of mineral species is governed by the species that occupies the cavities in the aluminosilicate framework as well as the type of crystal structure, either cubic or hexagonal. Nepheline is the basic NAS mineral with the formula $Na_2O$-$Al_2O_3$-$2SiO_2$. When sulfates are captured within the cage structure, nosean forms with the formula $3Na_2O$-$3Al_2O_3$-$6SiO_2$·$Na_2SO_4$. When chlorides are captured within the cage structure, sodalite forms with the formula $3Na_2O$-$3Al_2O_3$-$6SiO_2$·$2NaCl$. Depending on the waste compositions, process additives such as magnetite are added to retain Cr as $FeCr_2O_4$ (Jantzen et al., 2007). The retention of anions and cations within the mineral structures of the nepheline, sodalite, and nosean phases, as well as the role of magnetite, will be discussed here. The most comprehensive work on the subject has been performed by Jantzen et al. (2005) and Jantzen (2008) and this section summarizes the work presented there.

| Waste | Pilot-Scale Facility | Date | Sample ID | Monolith |
|---|---|---|---|---|
| **Hanford Wastes** | | | | |
| LAW AN-107, Envelope C [a], [b] | Hazen Research Facility, 6-inch FBSR | Dec. 2001 | SCT02-098-FM, Fines PR-01 | No |
| LAW Saltcake blend [c] | SAIC STAR, 6-inch FBSR | Aug. 2004 | Bed 1103, Bed 1104, Fines 1123 | Blend[i] |
| LAW Saltcake blend [d] | Hazen Research Facility, 15-inch FBSR | 2008 | P1 PR bed, HTF fines | Yes |
| WTP-SW LAW melter off-gas recycle [d] | Hazen Research Facility, 15-inch FBSR | 2008 | P2 PR bed, HTF fines | Yes |
| LAW Saltcake blend [e] | SRNL BSR, 2.75-inch | 2010 | Module B samples | No |
| WTP-SW LAW melter off-gas recycle [e] | SRNL BSR, 2.75-inch | 2010 | Module A samples | No |
| **Idaho Wastes** | | | | |
| SBW [f] | SAIC STAR, 6-inch FBSR | Jul-03 | Bed 260, Bed 272, Bed 277 | Blend[i] |
| SBW [g] | SAIC STAR, 6-inch FBSR | 2004 | Bed 1173 | Blend[i] |
| SBW [h] | Hazen Research Facility, 15-inch FBSR | 2004 | DMR4xxx, HTF4xxx | No |

(a) Jantzen, 2002
(b) Pareizs et al., 2005
(c) Olson et al., 2004a
(d) TTT, 2009
(e) Jantzen et al., 2011
(f) Marshall et al., 2003
(g) Olson et al., 2004b
(h) Ryan et al., 2008
(i) Blends are samples used in these studies that combined 20% LAW, 32% SBW and 45% starting bed material

Table 2. Summary of FBSR Pilot-Scale Sodium Aluminosilicate Waste Form Preparation Tests

The NAS mineral waste forms are comprised mostly of nepheline (nominally $NaAlSiO_4$ or $Na_3KAl_4SiO_{16}$) which is a hexagonal structured feldspathoid mineral, sodalite and nosean following the reactions:

$$\underbrace{2NaOH}_{\text{waste}} + \underbrace{Al_2O_3 \bullet 2SiO_2}_{\text{kaolinclayadditive}} \rightarrow 2\ \underbrace{NaAlSiO_4}_{\text{Nephelineproduct}} + H_2O \quad (1)$$

$$\underbrace{8NaOH + 2Cl}_{\text{waste}} + \underbrace{3(Al_2O_3 \bullet 2SiO_2)}_{\text{kaolinclayadditive}} \rightarrow \underbrace{Na_6Al_6Si_6O_{24}(2NaCl)}_{\text{Sodaliteproduct}} + 3H_2O + 2OH^- \quad (2)$$

$$\underbrace{8NaOH + SO_4}_{\text{waste}} + \underbrace{3(Al_2O_3 \bullet 2SiO_2)}_{\text{kaolinclayadditive}} \rightarrow \underbrace{Na_6Al_6Si_6O_{24}(Na_2SO_4)}_{\text{Nosean product}} + 3H_2O + 2OH^- \quad (3)$$

$$\underbrace{8NaOH + 2ReO_4^-}_{\text{waste}} + \underbrace{3(Al_2O_3 \bullet 2SiO_2)}_{\text{kaolinclayadditive}} \rightarrow \underbrace{Na_6Al_6Si_6O_{24}(2NaReO_4)}_{\text{Sodaliteproduct}} + 3H_2O + 2OH^- \quad (4)$$

$$\underbrace{6NaAlSiO_4}_{\text{nephelineproduct}} + \underbrace{2NaReO_4}_{\text{waste}} \rightarrow \underbrace{Na_6Al_6Si_6O_{24}(2NaReO_4)}_{\text{Sodalite}} \quad (5)$$

The ring-structured aluminosilicate framework of nepheline forms cavities which can be 8- or 9-coordinated. There are eight large (9-fold oxygen) coordination sites and six smaller (8-fold oxygen) sites. The larger 9-fold coordination sites ionically bond with Ca, K, and Cs and the smaller 8-fold sites ionically bond with Na (Deer et al., 1963). When K is the cation it is known as kalsilite ($KAlSiO_4$). In nature, the nepheline structure is known to accommodate Fe, Ti and Mg, as well (Deer et al., 1963). In addition, rare earth nephelines are known, e.g. $NaYSiO_4$, $Ca_{0.5}YSiO_4$, $NaLaSiO_4$, $KLaSiO_4$, $NaNdSiO_4$, $KNdSiO_4$, and $Ca_{0.5}NdSiO_4$, where the rare earth substitutes for Al in the structure (Barrer, 1982). A sodium-rich cubic structured nepheline with excess Na is also known, e.g. $(Na_2O)_{0.33}\ Na[AlSiO_4]$ and was found in a FBSR mineralized product (Jantzen, 2002, Pareizs et al, 2004). This nepheline structure has large cage-like voids in the structure where Na can bond ionically to 12 framework oxygens (Klingenberg & Felsche, 1986). This cage-structured nepheline has not been shown to occur in nature. Despite this, the large cage-like voids should be capable of retaining large radionuclides, especially monovalent anions such as $(ReO_4)^{-1}$ (Olson et al., 2004a). Likewise, $Na_2O$ deficient nepheline structures have been found in other FBSR mineralizing campaigns for INEEL alumina-rich SBW (Olson et al., 2005).

Structurally related to the aluminosilicate framework of nepheline is the sodalite group of minerals. Sodalite minerals have cage-like structures formed of aluminosilicate tetrahedra. The cage structures retain anions and/or radionuclides that are ionically bonded to the aluminosilicate tetrahedral and to sodium. The cage in sodalite is occupied by two sodium and two chlorine ions can be written as $Na_6[Al_6Si_6O_{24}] \cdot 2NaCl$ to highlight that the NaCl molecules are chemically bonded in the cavities. If the NaCl molecules are replaced by $Na_2SO_4$, $Na_2CO_3$ and NaOH the mineral names are known as nosean, natrodavyne, and basic sodalite, respectively. Sodalite minerals are known to accommodate Be in place of Al and $S_2$ in the cage structure, along with Fe, Mn, and Zn, e.g. danalite ($Fe_4[Be_3Si_3O_{12}]S$), helvite ($Mn_4[Be_3Si_3O_{12}]S$), and genthelvite ($Zn_4[Be_3Si_3O_{12}]S$) (Deer et al, 1963). These cage-structured sodalites are also found to retain Mo, Cs, Sr, B, Ge, I and Br (Buhl et al., 1989;

Deer et al., 1963; Fleet, 1989). Regardless of the oxidation state of sulfur during FBSR processing, the feldspathoid minerals can accommodate sulfur as either sulfate or sulfide. Although neither Cs nor Rb sodalites have been identified as phase pure end members, Cs and Rb are tolerated in the sodalite structure (Deer et al, 1963; Deer et al., 2004). In addition, non-naturally occurring Zeolite-A structures are known to form from the reaction of CsOH and RbOH with kaolin clay (Barrer et al., 1968).

Due to the flexibility of the sodalite, monovalent species such as $Cs^{+}$, $K^{+}$, $Ca_{0.5}$, $Sr_{0.5}$, etc. can substitute for $Na^{+}$, while $(SO_4)^{-2}$ , $(MoO_4)^{-2}$, $(AsO_4)^{-2}$, $(MnO_4)^{-1}$, and $(ReO_4)^{-1}$ [and thus presumably $(TcO_4)^{-1}$], can all substitute for the $Cl^{-}$ in the structure. In addition, $I^{-}$, $Br^{-}$, $OH^{-}$, and $NO_3^{-2}$ can all substitute for the $Cl^{-}$ atoms. In the above-listed oxyanions, the oxygens in the tetrahedral polyhedral around the metal provide the oxygen bonds for the tetrahedral $XO_4$ groups. These oxygen come from four of the six tetrahedra forming a ring along the body diagonal of the cubic unit cell (Hassan & Gruncy, 1984). Boron and beryllium can substitute for Al in a tetrahedral polyhedra in the sodalite structures as can Ti. Elements such as Fe and Zn can substitute for $Na^{+}$ (Deer et al., 2004; Hassan & Gruncy, 1984). Figure 3 shows the flexibility of sodalite to incorporate various species in its structure.

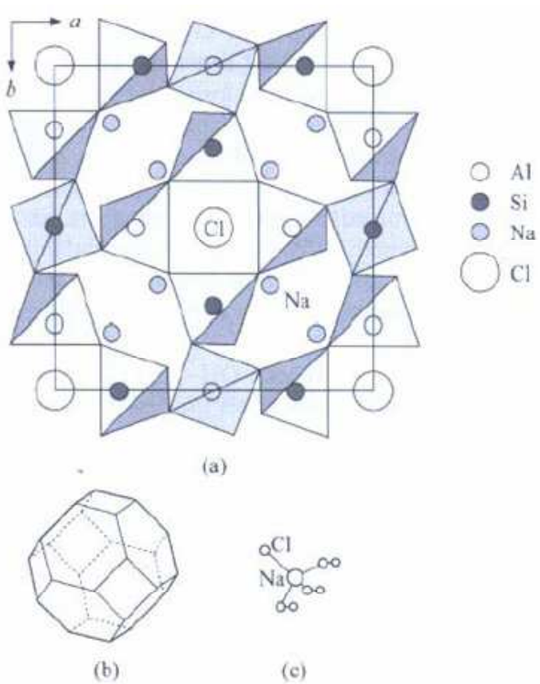



Fig. 3. Structure of Sodalite showing (a) two-dimensional projection of the (b) three-dimensional structure and (c) the four fold ionic coordination of the Na site to the $Cl^{-}$ ion and three framework oxygen bonds. (Deer et al., 2004)

The last of the mentioned feldspathoid cage-structured minerals is nosean, $Na_6[Al_6Si_6O_{24}](Na_2SO_4)$. Nosean has $Na_2SO_4$ bonded in the sodalite cage like structure. All bonding in the sodalite/nosean single unit cell is ionic and the atoms are regularly arranged. This is similar to the manner of ionic bonding in glass, but more highly ordered than the atomic arrangements in glasses which have no long-range order (Jantzen, 2008).

Another possible additive in FBSR processing to catalyze denitration is an iron oxide co-reactant containing the spinel mineral magnetite (Jantzen, 2002). In this situation, and potentially for waste streams rich in iron, spinels form that retain cations such as Cr within the structure as $FeCr_2O_4$. This incorporation is made possible due to the reduction of $Cr^{6+}$ to $Cr^{3+}$ at the elevated temperature and reducing atmosphere of the FBSR process (Jantzen et al., 2007). The spinels such as $Fe_3O_4$ ( $Fe^{+2}Fe_2^{+3} + O_4$) are known to take $Cr^{+3}$ and $Ti^{+3}$ into their lattice in place of $Fe^{+3}$, as well as many of the divalent transition metals like $Ni^{2+}$, $Mn^{2+}$, $Zn^{2+}$, and $Mg^{2+}$ (Deer et al., 1963). Spinels have both tetrahedral and octahedral coordination spheres with oxygen. The trivalent ions reside in the four-fold coordination positions and the divalent ions reside in the six-fold coordination positions. All the trivalent and divalent ions are ionically bonded to oxygen (Jantzen, 2008).

### 3.1.2 FBSR product morphology

The FBSR granular product is composed of two fractions from the FBSR process. Solids collected from the bottom of the fluidized bed are captured in the PR. Figure 4 shows a photograph of the PR material from the 2008 Hazen pilot-scale test with the Hanford LAW simulant. The PR material includes residual carbon from coal or wood products used in the FBSR as an energy source and as a reductant. Unreacted carbon can be removed by roasting at 525°C (Bullock et al., 2002). Carbon is often removed to ensure that it does not contribute to the measured surface area used for durability testing (Jantzen & Crawford, 2010). This temperature is high enough to remove carbon in an oxidizing atmosphere but not too high to change the composition of the phase assemblages of the product. The PR material may also include residual alumina used as an initial seed material when the FBSR is first started up. Solids leaving the FBSR entrained in the fluidizing gases are captured in the high-temperature filter (HTF). The morphology of the finer particles, which tend to clump together but are relatively easy to collect are also shown in Figure 4.

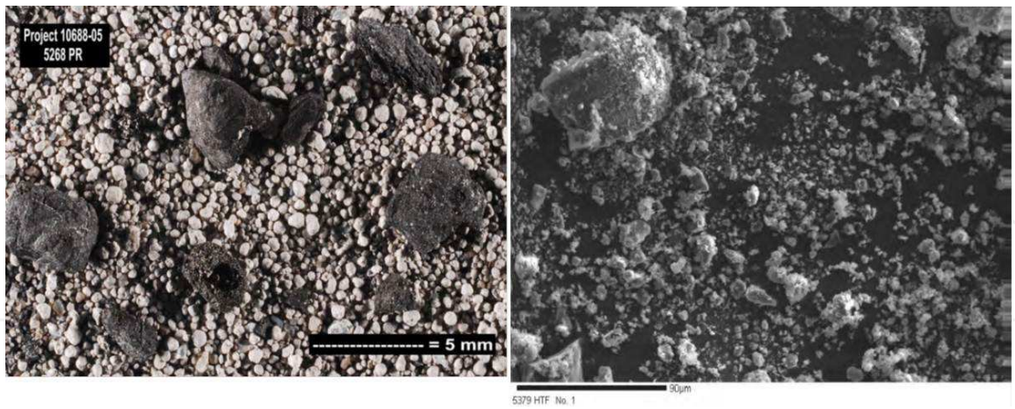



Fig. 4. Example of FBSR Granular Product from the Product Receiver (left). Microprobe Photographs of High Temperature Filter (HTF) Fines (right) (from TTT, 2009)

Some scanning electron microscopy (SEM) micrographs of the FBSR material from the 2001 Hazen Research facility test with Hanford LAW are presented in Figure 5. The micrograph on the left clearly shows FBSR materials to be highly porous. It is also worth noticing the black dots in the micrograph on the right which indicate the presence of magnetite ($Fe_3O_4$). Iron oxides are also good hosts for contaminants, e.g. forming spinels with Cr and Ni in the wastes.

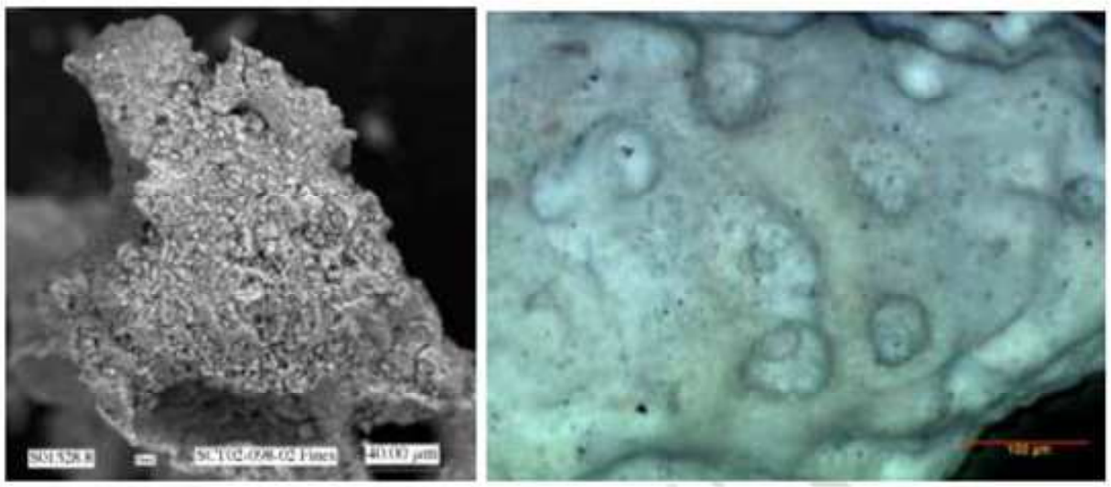
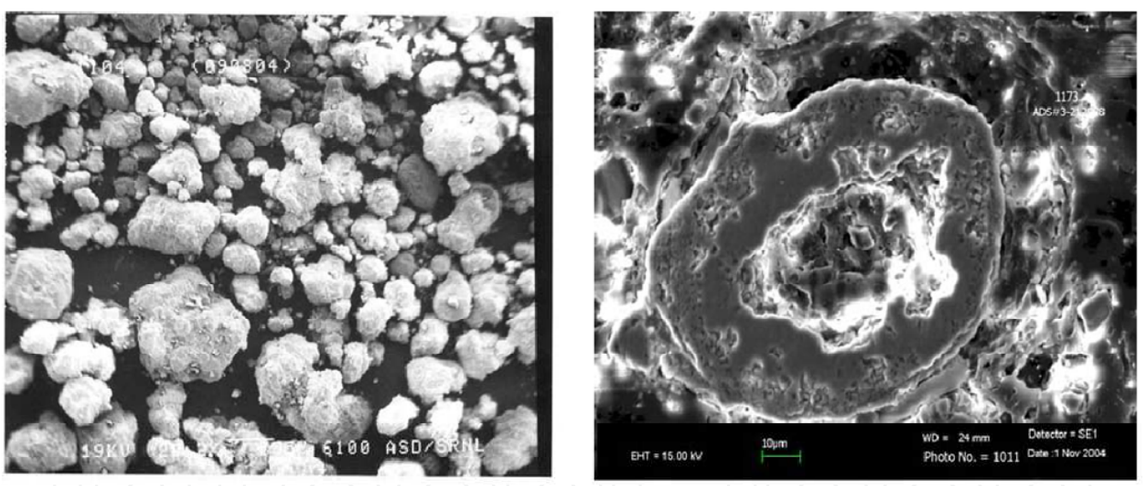


Fig. 5. SEM Micrographs of Typical FBSR Product Grain (left). Optical photograph of SCT02-098 particle (FBSR material); the black particles are magnetite ($Fe_3O_4$) (McGrail et al., 2003a).




**(a)** 1123 Bed product **(b)** 1173 Bed product (sectioned)

Fig. 6. SEM Photomicrographs of FBSR Bed Product Showing the Surface Topography and Porosity (Lorier et al., 2005). Also see Table 2 for sample origins.

Figure 6 shows SEM micrographs in as received (left) and in as embedded and sectioned (right) by Lorier et al. (2005) of FBSR materials from tests in 2004 with Hanford LAW saltcake simulant (Bed 1123) and INEEL SBW simulant (Bed 1173), respectively. The LAW saltcake FBSR product shows the particle shape and irregular surface topography of the granular product. The SBW micrograph shows the internal porosity of a granule in cross-section. Large uncertainties associated with the porosity of the FBSR granular product gives

a large discrepancy between a calculated geometric surface area and the measured surface area of the material using Brunauer, Emmett, and Teller (BET) (Brunauer et al., 1938) surface area measurements. Using the smaller surface area from the geometrical value would lead to an underestimation in dissolution rates used for product durability studies therefore it has been recommended to use the surface area obtained from BET measurements (McGrail et al., 2003a).

### 3.2 Phase composition and mineralogy

Studies have been conducted with different FBSR materials to determine the minerals that are present. Most of these minerals are believed to belong to the groups of nepheline, sodalite, and carnegieite, all feldspathoids with a one molar ratio of Si:Al:Na. Carnegeite is a metastable form of nepheline with the same chemical composition but with less atomic order. It readily transforms to nepheline upon heating (Jantzen & Crawford, 2010). Both nepheline and carnegeite have ring structures. In Table 3 one may see a summary of the mineral phases identified by Jantzen and Crawford (2010) in the Hanford LAW and WTP-SW pilot-scale tests as well as the INEEL SBW tests. Nepheline ($NaAlSiO_4$) is the primary phase formed. The fines captured in the HTF have a shorter residence time in the FBSR and contain low-carnegieite. Data in the table are from an XRD method that gives information on the specific crystalline phases present by comparison to reference library spectra. No internal standards were used to allow for quantitative measurements of the phases. Information on 'major,' 'minor' and 'trace' phases present are given by intercomparison of the main peaks of each crystalline pattern within a sample.

In addition to the NAS phases, other minor phases have been identified using XRD of the FBSR granular product. These include quartz ($SiO_2$) and anatase ($TiO_2$), which are impurities in the clays used as mineralizing agents in the FBSR. Corundum (crystalline alumina, $Al_2O_3$) results from the seed material for starting up the FBSR process. Its concentration decreases over time as the starting FBSR bed material leaves through the PR. Hematite ($Fe_2O_3$) and magnetite ($Fe_3O_4$) were identified in the Hanford Envelope C product, most likely due to the iron oxide additive used as a denitration catalyst (Jantzen, 2002). Jantzen et al. (2006b) also report that amorphous metakaolin was identified by SEM in the early LAW Envelope C and Envelope A FBSR tests as unreacted cores in the mineralized granules.

Nosean and sodalite have been identified as minor NAS phases in the FBSR granular product. Nosean and sodalite have cage structures that can retain anions and radionuclides that bond ionically within the structure. Table 4 shows how various elements within Hanford tank wastes may substitute in the nepheline, sodalite, and nosean structures (Jantzen et al., 2011).

The oxidation state can impact how and where contaminants are captured in the FBSR product (Jantzen, 2008). The FBSR process is run under reducing conditions with a log oxygen fugacity of -15 to -16 Pa. Under the designed REDOX conditions, a REDOX-sensitive species, such as chromium, is predicted to be 50 to 70% reduced to $Cr^{3+}$ and would be sequestered in a spinel (hematite or magnetite) phase. Sulfur is predicted to be only 1 to 19% reduced to $S^{2+}$ and would enter the sodalite phase as $SO_4$ in the +6 oxidation state.

| FBSR Product | Low-Carnegieite[a] | Nepheline | Nosean and/or Sodalite | Other Minor Components |
|---|---|---|---|---|
| **Hanford Envelope "C" LAW Wastes (2002) $Fe^{+2}/\Sigma Fe$ of Bed = 0.15** | | | | |
| SCT02-098-FM | | X | Y | $Al_2O_3$, $Fe_2O_3$, $Fe_3O_4$ |
| Fines PR-01 | X | X | Y | $Al_2O_3$, $Fe_2O_3$, $Fe_3O_4$ |
| **Hanford Envelope "A" LAW Wastes (2004) $Fe^{+2}/\Sigma Fe$ of Bed = 0.28-0.81** | | | | |
| Bed 1103 | X | X | Y | $TiO_2$ |
| Bed 1104 | X | X | Y | $TiO_2$ |
| Fines 1125 | X | Y | | $TiO_2$ |
| **INEEL SBW Wastes (2003-2004) $Fe^{+2}/\Sigma Fe$ of Bed = 0.51-0.61** | | | | |
| Bed 260 | Y | X | TR | $Al_2O_3$ and $TiO_2$ |
| Bed 272 | Y | X | TR | $TiO_2$ |
| Bed 277 | Y | X | TR | $TiO_2$ |
| Bed 1173 | | X | TR | $Al_2O_3$, $SiO_2$, $NaAl_{11}O_{17}$, $(Ca,Na)SiO_3$ |
| **Hanford Rassat LAW Wastes (2008) $Fe^{+2}/\Sigma Fe$ of Bed = 0.41-0.90** | | | | |
| PR Bed Product 5274 (P1A) | Y | X | X | $Al_2O_3$ |
| PR Bed Product 5316 (P1A) | Y | X | X | Pyrophyllite* |
| HTF Fines 5280 (P1A) | X | Y | | $NaAl_{11}O_{17}$ (Diaoyudaoite),$TiO_2$ |
| HTF Fines 5297 (P1A) | X | Y | X | $SiO_2$ |
| PR Bed Product 5359 (P1B) | Y | X | X | Pyrophyllite* |
| PR Bed Product 5372 (P1B) | Y | X | X | Pyrophyllite* |
| HTF Fines 5351 (P1B) | X | Y | Y | $SiO_2$ |
| HTF Fines 5357 (P1B) | X | Y | Y | $TiO_2$ |
| Composite (P1A) | X | Y | Y | $SiO_2$ and $TiO_2$ |
| Composite (P1B) | X | Y | Y | $SiO_2$ and $TiO_2$ |
| **Hanford Melter Off-Gas Recycle (WTP SW) Wastes (2008) $Fe^{+2}/\Sigma Fe$ =0.41-0.90** | | | | |
| PR 5475 (P2A) | Y | Y | X | Pyrophyllite* |
| HTF Fines 5471 (P2A) | X | X | X | $SiO_2$ |
| PR 5522 (P2B) | Y | Y | X | Pyrophyllite*, $TiO_2$ |
| HTF Fines 5520 (P2B) | X | X | X | $SiO_2$ and $TiO_2$ |
| Composite (P2B) | Y | X | X | $SiO_2$ |

X = Major constituent; Y = Minor constituent; TR = trace constituent; a = the PDF for this phase states it is orthorhombic nepheline and possibly low-carnegeite (PDF 052-1342). Note low-carnegeite also has ring structures that are oval for sequestration of K, Cs, etc; *$Al_{1.333}Si_{2.667}O_{6.667}(OH)_{1.333}$

Table 3. Mineral Phases Analyzed in FBSR Products (from Jantzen & Crawford, 2010).

Rhenium, often used as a non-radioactive surrogate for technetium, is predicted to be only 2 to 6% reduced to the +4 oxidation state at the nominal operating conditions. At the +7 oxidation state, rhenium, and by association, technetium, are predicted to enter the sodalite phase. Mattigod et al. (2006) were able to synthesize sodalite [$Na_8$ $(AlSiO_4)_6(ReO_4)_2$] that contained Re(VII). Its crystal structure was determined from Rietveld refinement of

experimental XRD data. This study showed that Re(VII) can be incorporated into NAS solids. REDOX control is important for making certain that the contaminants enter the desired FBSR mineral phases. Only 2.5% of the Re was in the +7 state and 1% of the S was in the +6 state in the HTF product compared to 94 to 95% Re(VII) and 86 to 89% $S^{6+}$ in the PR product.

| Nepheline—Kalsilite Structures (a) | Sodalite Structures (b) | Nosean Structures |
|---|---|---|
| $Na_xAl_ySi_zO_4$ (c) where x=1-1.33 y and z = 0.55-1.1 | $[Na_6Al_6Si_6O_{24}](NaCl)_2$ (c) | $[Na_6Al_6Si_6O_{24}](Na_2SO_4)$ (c, d) |
| $KAlSiO_4$ | $[Na_6Al_6Si_6O_{24}](NaF)_2$ (c) | $[Na_6Al_6Si_6O_{24}](Na_2Mo_4)$ (c, e) |
| $K_{0.25}Na0._{75}AlSiO_4$ (c) | $[Na_6Al_6Si_6O_{24}](NaI)_2$ (d) | $[Na_6Al_6Si_6O_{24}]((Ca,Na)SO_4)_{1-2}$ (f) |
| $CsAlSiO_4$ (c) | $[Na_6Al_6Si_6O_{24}](NaReO_4)_2$ (g) | $[(Ca,Na)_6Al_6Si_6O_{24}]((Ca,Na)S,SO_4,Cl)$ |
| $RbAlSiO_4$ (c) | $[Na_6Al_6Si_6O_{24}](NaMnO_4)_2$ (h) | |
| $(Ca_{0.5},Sr_{0.5})AlSiO_4$ (c) | $(NaAlSiO_4)_6(NaBO_4)_2$ (i, j) | |
| $(Sr,Ba)Al_2O_4$ (c) | $Mn_4[Be_3Si_3O_{12}]S$ (d) | |
| $KFeSiO_4$ (c) | $Fe_4[Be_3Si_3O_{12}]S$ (d) | |
| $(Na,Ca_{0.5})YSiO_4$ (h) | $Zn_4[Be_3Si_3O_{12}]S$ (d) | |
| $(Na,K)LaSiO_4$ (h) | | |
| $(Na,K,Ca_{0.5})NdSiO_4$ (h) | | |

(a) Iron, $Ti^{3+}$, Mn, Mg, Ba, Li, Rb, Sr, Zr, Ga, Cu, V, and Yb all substitute in trace amounts in nepheline (Deer et al., 2004).
(b) Higher valent anionic groups such as $AsO_4^{3-}$ and $CrO_4^{2-}$ form $Na_2XO_4$ groups in the cage structure where X= Cr, Se, W, P, V, and As (Barrer, 1982).

(c) Deer et al., 2004 (f) Dana, 1931 (i) Buhl et al. 1989
(d) Deer et al., 1963 (g) Mattigod et al., 2006 (j) Tobbens and Buhl 2000
(e) Brookins 1984 (h) Barrer 1982

Table 4. Cation and Anion Substitution in Feldspathoid Mineral Structures (from Jantzen et al., 2011)

### 3.3 Encapsulating materials

The FBSR granular product will need to be encapsulated in a binder or be contained within high-integrity containers to meet Hanford IDF requirements for compressive strength of 3.4 MPa (500 psi). The compressive strength requirement is driven by the need to prevent subsidence, or sinking, of the disposal facility to maintain surface cap and barrier functionality. Encapsulating the granular product also helps reduce the impact of the dispersible materials in human intrusion scenarios.

Several works have studied the encapsulation of the FBSR granular products with various binders (Jantzen, 2006, 2007; TTT, 2009). Different matrices that have been evaluated as potential binders for FBSR granular product encapsulation have been ordinary Portland

cement (OPC), Ceramicrete phosphate bonded ceramic, hydroceramic cements, and several geopolymers. The cement monoliths were prepared with Type II Portland cement and Portland cement plus precipitated silica as a chemically pure representative of a fly ash pozzolanic material. Ceramicrete is a phosphate-based cement developed at Argonne National Laboratory (ANL) (Singh et al., 1997, 1998; Wagh et al., 1997, 1999). It is made from an acidic solution of potassium dihydrogen phosphate ($KH_2PO_4$) and magnesium oxide (MgO). Hydroceramics are prepared through the reaction of a sodium hydroxide solution with metakaolin clay. Under controlled curing conditions, the clay and caustic react to form zeolite mineral phases. Geopolymers are amorphous ceramic-like, inorganic polymers made from the cross-linked three-dimensional structure of aluminosilicates. No zeolite phases form because of the insufficient presence of water. All binders are formed at room temperature. The monoliths must be able to include the FBSR granular bed product material, the starting bed product, HTF fines, and unreacted carbon. Comparisons of some different binder materials can be seen in Table 5.

| Binder Type | Monolith | Waste Loading | Compressive Strength (psi) | Cure Time (days) | Density (g/cc) | BET Surface area (m2/g) |
|---|---|---|---|---|---|---|
| OPC | OPC-1 | 80% | 1,630 | 12 | 1.64 | 31.5 |
| OPC | OPC-2 | 87% | 573 | 28 | 1.61 | 21.3 |
| High Al Cement | FON-1 | 68% | 770 | 7 | 1.77 | 20 |
| High Al Cement | FON-2 | 74.16% | 490 | 7 | 1.75 | 15.5 |
| High Al Cement | S41-1 | 68.60% | 672 | 7 | 1.75 | 10.7 |
| High Al Cement | S41-2 | 74.16% | 340 | 15 | 1.7 | 10.7 |
| High Al Cement | S71-1 | 68.60% | 1,120 | 7 | 1.7 | 13.1 |
| High Al Cement | S71-2 | 74.16% | 550 | 15 | 1.65 | 9.2 |
| Geopolymer | GEO-1 | 67% | 1,510 | 11 | 1.87 | 15.2 |
| Geopolymer | GEO-2 | 72% | 860 | 14 | 1.87 | 17.3 |
| Geopolymer | GEO-3 | 67% | 1,270 | 11 | 1.81 | 10.9 |
| Geopolymer | GEO-4 | 71% | 410 | 11 | 1.84 | 6.2 |
| Geopolymer | GEO-5 | 63% | 950 | 7 | 1.88 | 10.6 |
| Geopolymer | GEO-6 | 66% | 1,080 | 7 | 1.82 | 10 |
| Ceramicrete | CER-1 | 67% | 520 | 8 | 1.81 | 32.2 |
| Ceramicrete | CER-2 | 73% | 550 | 28 | 1.81 | 27.7 |

Table 5. A summary of 2-inch Monolith Cubes (TTT, 2009).

## 4. Physical properties

Table 6 gives data on the density, particle size, and surface area of the FBSR granular product from the early FBSR campaigns with INEEL SBW and the Hanford LAW campaign (Jantzen et al., 2006). The measured BET surface areas were measured in this study on a carbon-free basis (coal removed by roasting), and the value measured by McGrail et al. (2003a) (coal removed manually) was obtained for comparison. The geometric surface area is from Lorier et al. (2005).

| | Density by Pycnometry ($g/cm^3$) | Surface Area by BET ($m^2/g$) | Surface Area Geometric ($m^2/g$) |
|---|---|---|---|
| **SBW SAIC STAR (Marshall et al., 2003)** | | | |
| Bed 260, 272, 277 | 3.30, 3.13, 2.73 | 6.03 | |
| **LAW Saltcake (Rassat blend) SAIC STAR (Olson et al. , 2004a)** | | | |
| Bed 1103 | 2.53 | 4.53 | |
| Bed 1123 | 2.53 | 4.43 | 0.0212[a] |
| Fines 1125 | 2.46 | 4.41 | |
| **SBW Hazen (Olson et al., 2004b)** | | | |
| Bed 1173 | 2.76 | 2.36 | 0.0194[a] |
| **LAW Envelope C (AN-107) Hazen (Jantzen, 2002; Pareizs et al., 2005)** | | | |
| Bed SCT-02 | 2.66, 2.764[b] | 2.37[b] | 0.0193 |
| PR-01 Fines | 2.5 | 5.15 | |

(a) Lorier et al., 2005
(b) McGrail et al., 2003b

Table 6. Density and Surface Area of FBSR Granular Products

## 5. Contaminant release mechanisms

A current summary of knowledge regarding the mineralization of radioactive wastes by the FBSR process and a comparison of the durability glass and the FBSR mineral phases has been provided in a previous publication by Jantzen (2008). A basic understanding of FBSR contaminant release mechanisms starts with an understanding of the crystalline product. Mineral waste assemblages formed by FBSR possess short-range order (SRO). SRO in the NAS mineral structures allows contaminants to be trapped in the cage-shaped structures while those external to the cage-shaped structures are bound ionically to oxygen atoms. NAS cage-structured feldspathoid minerals present in FBSR material (mostly sodalite, nosean, and nepheline) are formed by SRO. SRO becomes medium-range order (MRO) through the structures of $(SiO_4)^{-4}$ and $(AlO_4)^{-5}$ tetrahedra, which are joined by sharing one or more of the four oxygen atoms with another tetrahedra. The tetrahedra are arranged to form a cage (sodalite, nosean) or rings (nepheline) via one or two of the tetrahedral oxygen atoms (bridging oxygens), while the other tetrahedral oxygen atoms (non-bridging oxygens) are available to bond ionically with the cations inside or outside the cage. These cations may be alkali or alkaline earths which may be hazardous or radioactive. The cage and/or ring structures are repeated at regular periodicity, which is the long-range order (LRO) characteristic of mineral/crystalline structures. The LRO provides shorter and more regular oxygen-cation (ionic) bonding and a periodic ordering. Glasses do not possess LRO, but they do possess SRO and MRO. Sometimes glasses have more highly ordered regions, referred to as clusters or quasicrystals that have atomic arrangements that approach those of crystals. The ordered regions are metastable compared to crystalline minerals because crystalline species are at their lowest thermodynamic free energy. Therefore, the NAS FBSR mineral structure waste forms are inherently stable.

An explanation of the enhanced durability has been given by Jantzen (2008). According to this author, the dissolution mechanisms (contaminant release mechanisms) of the SRO and MRO in mineral (ceramic) and vitreous waste forms are similar. Mineral waste forms can afford better retention of cationic species compared to glass waste forms due to the LRO of

the mineral structure and the regularity of the coordination and bonding of a given coordination polyhedra in which a cation or radionuclide resides. While the activation energy required to break an Si-O, Al-O, B-O bond may be similar in a glass and a ceramic/mineral, due to the SRO, the $(SiO_4)^{-4}$, $(BO_4)^{-5}$, $(BO_3)^{-3}$ and some $(AlO_4)^{-5}$ are more rigidly retained in a mineral structure due to the LRO and periodicity (repeated pattern) of the polyhedra. This author also asserts that in mineral waste forms, as in glass, the molecular structure controls contaminant release by establishing the distribution of ion exchange sites, hydrolysis sites, and the access of water to those sites. It has been demonstrated experimentally that ion exchange in glass occurs along percolation channels that exist in glass. The cations in the percolation channels are ionically bonded to the non-bridging oxygen (NBO) bonds, just as they are in the more ordered crystalline mineral species. In the mineral waste forms there are no percolation channels and dissolution with water must attack the ionically bonded lattice from the surface. The basic difference is that there may be fewer bonds around a given cation in a glass or the bonds may have varying lengths compared to those in a crystalline or mineral waste form.

## 6. Concluding remarks

The primary product from the FBSR process is a granular product composed of NAS minerals. The NAS FBSR granular product is a multiphase mineral assemblage of Na-Al-Si feldspathoid minerals (sodalite, nosean, and nepheline) with cage and ring structures that sequester anions and cations (Jantzen et al., 2007). Nepheline is the basic NAS mineral with the formula $Na_2O$-$Al_2O_3$-$2SiO_2$. When sulfates are captured within the cage structure, nosean forms with the formula $3Na_2O$-$3Al_2O_3$-$6SiO_2$·$Na_2SO_4$. When chlorides are captured within the cage structure, sodalite forms with the formula $3Na_2O$-$3Al_2O_3$-$6SiO_2$·2NaCl. Depending on the waste compositions, process additives such as magnetite are included to form iron-bearing spinel minerals to sequester Cr and Ni in the waste.

The FBSR waste form may be encapsulated in a binder to minimize dispersability. A number of binders have been evaluated including ordinary Portland cement, high-alumina cements, geopolymers prepared with either kaolin clay or fly ash, various hydroceramic cements and an advanced silicone geopolymer composite material. Characterization data are available on the FBSR granular product prepared with the LAW, WTP-SW, and SBW simulants. This includes some contaminant release studies to support risk assessments and LAW waste form down selections in the early 2000's. Some characterization data is also available on the various binders being evaluated.

### 6.1 Strengths associated with this waste form

Fluidized Bed Steam Reforming (FBSR) offers a moderate temperature continuous method by which LAW and/or WTP-SW wastes can be processed irrespective of whether they contain organics, nitrates, sulfates/sulfides, chlorides, fluorides, volatile radionuclides or other aqueous components. The FBSR technology can process these wastes into a crystalline ceramic (mineral) waste form. The FBSR process also differs from glass or ceramic waste form production in that it is carried out at temperatures ranging from 700 to 750°C whereas glass are ceramics are made from temperatures ranging from 1000 to 1500°C (Jantzen, 2008; Vora et al., 2009; Williams et al., 2010). This makes FBSR an attractive option in secondary liquid waste treatment especially for encapsulation of volatile contaminants of concern.

Monolithing of the granular FBSR product is being investigated to prevent dispersion during transport or burial/storage, which is a regulatory driver and not necessary for the durability and performance of this waste form. The mineral product degrades by the breaking of atomic bonds in the mineral structure in the same fashion as atomic bonds are broken in vitreous waste forms. Therefore, monolith formulation versus durability is considered supplementary since monolith selection is based on the scenario that the monolith will not compromise the mineral product durability.

The FBSR process has been demonstrated at a non-radioactive scale using simulants for Hanford LAW wastes and Idaho SBW. The FBSR process has been demonstrated with a secondary waste stream (WTP-SW) from the WTP based on an early LAW scenario in which the LAW melter submerged bed scrubber and wet electrostatic precipitator condensates are sent from the WTP as a secondary liquid stream for treatment. A testing program is currently underway using a bench-scale steam reformer and actual tank wastes.

Research teams from SRNL and PNNL are currently working to perform different tests with the FBSR materials. Some of the major findings and results collected so far and are summarized below:

- Data indicates $^{99}$Tc, Re, Cs, and I (all isotopes) report to the mineral product and not to the off-gas
- $^{99}$Tc and Re show similar behavior in partitioning between product and off-gas
- $^{99}$Tc, Re, $SO_4$ and Cr behavior are controlled by the oxygen fugacity in the FBSR/BSR process, i.e. control of the REDuciton/OXidation (REDOX) equilibrium
- XAS results show that Re is in the 7+ oxidation state and contained in the sodalite structure
- Re is a good surrogate for $^{99}$Tc during leaching experimentation proving that the current radioactive and simulant BSR campaign products using Re and $^{99}$Tc match the historic and engineering scale data that used Re only proving the "tie back" strategy
- All monoliths made from radioactive and non-radioactive granular products pass compression testing at >3.4 MPa (500 psi), maintain PCT leach rates <2 g/m$^2$, and perform well in ASTM C1308 (ASTM, 2008b) and ANSI 16.1 (ANS, 2008) testing indicating that the binder material is not degrading the granular product durability response.
- In order to match the Bench-Scale Reformer (BSR) REDOX to the Engineering Scale Technology Demonstration (ESTD) REDOX, the addition of reductants such as coal and control of gas inputs were adjusted during production: a more rigorous REDOX control strategy needs to be developed to ensure the COCs are in the correct oxidation states.

### 6.2 Sparse data and unresolved issues

Though the FBSR products have been studied over the last years, there are still some areas that remain with sparse data and unresolved issues. This is in contrast with glasses that have been studied as confinement materials for more than 30 years. More durability testing of all FBSR products using both the Single Pass Flow-Through (SPFT) and Product Consistency Test (PCT) methods to compare to various glasses are needed to better understand contaminant release mechanisms. The physical characteristics of the FBSR material must also be studied. This includes a better standing of the effective surface area

available for leaching by water. Further research needs to be conducted to determine the preferred host mineral phase for different radioactive materials and COCs under oxidizing and reducing conditions. Data must be obtained regarding the impacts of radiation, biodegradation, and water immersion on the compressive strength of the FBSR granular product encapsulated in any of the binder materials being considered for compression tests. Methods to consolidate the FBSR granular product into monolith waste forms are being investigated (Jantzen, 2007; TTT, 2009). The porosity and void volume of these materials on an engineering or production scale are, as yet, unknown. More research also needs to be conducted concerning the fabrication of the binder.

## 7. References

ANS—American Nuclear Society (2008). Measurement of the Leachability of Solidified Low-Level Radioactive Wastes by a Short-Term Test Procedure. *ANSI/ANS-16.1-2003; R2008,* American Nuclear Society, La Grange Park, Illinois.

ASTM—American Society for Testing and Materials (2008a). Standard Test Method for Determining the Chemical Durability of Nuclear Waste Glasses: The Product Consistency Test (PCT). *ASTM C1285 - 02(2008),* American Society for Testing and Materials, West Conshohocken, Pennsylvania.

ASTM—American Society for Testing and Materials (2008b). Standard Test Method for Accelerated Leach Test for Diffusive Releases from Solidified Waste and a Computer Program to Model Diffusive, Fractional Leaching from Cylindrical Waste Forms. *ASTM C1308-08,* American Society for Testing and Materials, West Conshohocken, Pennsylvania.

Barrer, R.M. (1982). *Hydrothermal Chemistry of Zeolites.* Academic Press, ISBN: 0120793601, New York

Barrer, R.M, Cole, J.F., & Sticher. H. (1968). Chemistry of Soil Minerals. Part V, Low Temperature Hydrothermal Transformations of Kaolinite. *Journal of the Chemical Society A: Inorganic, Physical, Theoretical,* pp. 2475-2485

Baumann, E.W. (1992). Colorimetric Determination of Iron(II) and Iron(III) in Glass. *Analyst*, Vol. 117, No. 5, pp. 913-916

Brunauer, S., Emmett, P.H., & Teller, E. (1938). Adsorption of Gases in Multimolecular Layers. *Journal of the American Chemical Society,* Vol. 60, pp. 309-319

Buhl, J.C, Engelhardt, G., & Felsche, J. (1989). Synthesis, X-Ray Diffraction, and MAS n.m.r. Characteristics of Tetrahydroxoborate Sodalite, $Na_8[AlSiO_4]_6[B(OH)_4]_2$. *Zeolites,* Vol. 9, No. 1, pp. 40-44

Bullock Jr, J.H., Cathcart, J.D., & Betterton. W.J. (2002). Analytical methods utilized by the United States Geological Survey for the analysis of coal and coal combustion by-products. *Open-File Report 02-389*. U. S. Geological Survey, Denver, Colorado.

Burket, P.R., Daniel, W.E., Nash, C.A., Jantzen, C.M. & Williams, M.R. (2008). Bench-Scale Steam Reforming of Actual Tank 48H Waste. *SRNS-STI-2008-00105*, Savannah River National Laboratory, Aiken, South Carolina.

Crawford, C.L. & Jantzen, C.M. (2007). Durability Testing of Fluidized Bed Steam Reformer (FBSR) Waste Forms for Sodium Bearing Waste (SBW) at Idaho National Laboratory (INL). *WSRC-STI-2007-00319*, Savannah River National Laboratory, Aiken, South Carolina.

Dana, E.S. (1932). *A Textbook of Mineralogy,* ISBN: 9780471193050, John Wiley & Sons, Inc., New York

Deer, W.A., Howie, R.A., & Zussman, J. (1963). *Rock-Forming Minerals*. ISBN: 9781862392595, John Wiley & Sons, Inc., New York

Deer, W.A., Howie, R.A., Wise, W.S., & Zussman, J. (2004). *Rock-Forming Minerals, Framework Silicates: Silica Minerals, Feldspathoids and the Zeolites*. ISBN: 9781862391444, The Geological Society, London

Fleet, M.E. (1989). Structures of sodium alumino-germanate sodalites. *Acta Crystallographica C: Crystal Structure Communications C*, Vol. 45, No. 6, pp. 843-847

Hassan, I. & Gruncy, H.D. (1984). The Crystal Structures of Sodalite-Group Minerals. *Acta Crystallography Section B,* Vol. 40, No. 1, pp. 6-13

Jantzen, C.M. (2002). Engineering Study of the Hanford Low Activity Waste (LAW) Steam Reforming Process (U). *WSRC-TR-2002-00317, Rev. 1*, Savannah River National Laboratory, Aiken, South Carolina.

Jantzen, C.M. (2006). Fluidized Bed Steam Reformer (FBSR) Product: Monolith Formation and Characterization. *WSRC-STI-2006-00033*, Savannah River National Laboratory, Aiken, South Carolina.

Jantzen, C.M. (2007). Fluidized Bed Steam Reformer (FBSR) Monolith Formation, *Proceedings of Waste Management 2007*, Tucson, Arizona, March 2007.

Jantzen, C.M. (2008). Mineralization of Radioactive Wastes by Fluidized Bed Steam Reforming (FBSR): Comparisons to Vitreous Waste Forms, and Pertinent Durability Testing. *WSRC-STI-2008-00268*, Savannah River National Laboratory, Aiken, South Carolina.

Jantzen, C.M & Crawford, C.L. (2010). Mineralization of Radioactive Waste Wastes by Fluidized Bed Steam Reforming (FBSR): Radionuclide Incorporation, Monolith Formation, and Durability Testing. *Proceedings of Waste Management 2010*, Phoenix, Arizona, March 2010.

Jantzen, C.M., Pareizs, J.M., Lorier, T.H., & Marra, J.C. (2005). Durability Testing of Fluidized Bed Steam Reforming (FBSR) Products (U). *Proceedings of Waste Management Technologies in Ceramic and Nuclear Industries*, American Ceramic Society, Westerville, Ohio.

Jantzen, C.M., Lorier, T.H., Marra, J.C., & Pareizs, J.M. (2006). Durability Testing of Fluidized Bed Steam Reforming (FBSR) Waste Forms. *Proceedings of Waste Management 2006.* Tucson, Arizona, February 2006

Jantzen, C.M., Lorier, T.H., Pareizs, J.M., & Marra, J.C. (2007). Fluidized Bed Steam Reformed (FBSR) Mineral Waste Forms: Characterization and Durability Testing. In: *Scientific Basis for Nuclear Waste Management XXX,* eds. Begg, B., Dunn, D. S., Poinssot, C., 985: pp. 379-386. Materials Research Society, Warrendale, Pennsylvania.

Jantzen, C.M., Crawford, C.L., Burket, P.R., Daniel, W.G. Cozzi, A.D., & Bannochie, C.J. (2011). Radioactive Demonstrations of Fluidized Bed Steam Reforming (FBSR) as a Supplemental Treatment for Hanford's Low-Activity Waste (LAW) and Secondary Wastes (SW). *Proceedings of Waste Management 2011*, Phoenix, Arizona, February 2011

Klingenberg, R. & Felsche, J. (1986). Interstitial Cristobalite-Type Compounds $(Na_2O)_{0.33}Na[AlSiO_4]$). *Journal of Solid State Chemistry,* Vol. 61, No. 1, pp. 40-44.

Kyritsis, K., Meller, N. & Hall, C. (2009). Chemistry and Morphology of Hydrogarnets formed in Cement-Based CASH Hydroceramics Cured at 200° to 350°C. *Journal of the American Ceramic Society,* Vol. 92, No. 5, pp. 1105-1111

Lockrem, L. L. (2005). Hanford Containerized Cast Stone Facility Task 1 – Process Testing and Development Final Test Report, *RPP-RPT-26742, Rev. 0*, CH2M HILL Hanford Group, Inc., Richland, Washington.

Lorier, T.H., Pareizs, J.M., & Jantzen. C.M. (2005). Single-Pass Flow Through (SPFT) Testing of Fluidized-Bed Steam Reforming (FBSR) Waste Forms. *WSRC-TR-2005-00124*, Savannah River National Laboratory, Aiken, South Carolina.

Marshall, D.W., Soelberg, N.R., & Shaber, K.M. (2003). THOR® Bench-Scale Steam Reforming Demonstration. *INEEL/EXT-03-00437*, Idaho National Engineering and Environmental Laboratory, Idaho Falls, Idaho.

Mason, J.B., McKibbin, J., Ryan, K., & Schmoker, D. (2003). Steam Reforming Technology for Denitration and Immobilization of DOE Tank Wastes. *Proceedings of Waste Management 2003,* Tucson, Arizona, February 2003

Mattigod, S.V., McGrail, B.P., McCready, D.E., Wang, L.-Q., Parker, K.E., & Young, J.S. (2006). Synthesis and Structure of Perrhenate Sodalite. *Microporous and Mesoporous Materials,* Vol. 91, No. 1-3, pp. 139-144

McGrail, B.P., Pierce, E.M., Schaef, H.T., Rodriguez, E.A., Steele, J.L., Owen, A.T., & Wellman, D.M. (2003a). Laboratory Testing of Bulk Vitrified and Steam Reformed Low-Activity Waste Forms to Support a Preliminary Risk Assessment for an Integrated Disposal Facility. *PNNL-14414*, Pacific Northwest National Laboratory, Richland, Washington.

McGrail, B.P., Schaef, H.T., Martin, P.F., Bacon, D.H., Rodriguez, E.A., McCready, D.E., Primak, A.N,. & Orr, R.D. (2003b). Initial Evaluation of Steam-Reformed Low Activity Waste for Direct Land Disposal. *PNWD-3288*, Pacific Northwest Division, Richland, Washington.

Nimlos, M.R. & Milne, T.A. (1992). Direct Mass-Spectrometric Studies of the Destruction of Hazardous Wastes. 1. Catalytic Steam Re-Forming of Chlorinated Hydrocarbons. *Environmental Science & Technology,* Vol. 26, No. 3, pp. 545-552

Olson, A.L., Soelberg, N.R., Marshall, D.W., & Anderson, G.L. (2004a). Fluidized Bed Steam Reforming of Hanford LAW Using THOR® Mineralizing Technology. *INEEL/EXT-04-02492*, Idaho National Engineering and Environmental Laboratory, Idaho Falls, Idaho.

Olson, A.L., Soelberg, N.R., Marshall, D.W., & Anderson, G.L. (2004b). Fluidized Bed Steam Reforming of INEEL SBW Using THOR® Mineralizing Technology, *INEEL/EXT-04-02564*, Idaho National Engineering and Environmental Laboratory, Idaho Falls, Idaho.

Olson, A.L., Soelberg, N.R., Marshall, D.W., & Anderson, G.L. (2005). Mineralizing, Steam Reforming Treatment of Hanford Low-Activity Waste. *Proceedings of Waste Management 2005,* Tucson, Arizona, February 2005

Pareizs, J.M., Jantzen, C.M., & Lorier, T.H. (2005). Durability Testing of Fluidized Bed Steam Reformer (FBSR) Waste Forms for High Sodium Wastes at Hanford and Idaho (U). *WSRC-TR-2005-00102*, Savannah River National Laboratory, Aiken, South Carolina.

Russell, R.L., Schweiger, M.J., Westsik Jr, J.H., Hrma, P.R., Smith, D.E., Gallegos, A.B., Telander, M.R., & Pitman, S.G. (2006). Low Temperature Waste Immobilization

Testing. *PNNL-16052 Rev 1*, Pacific Northwest National Laboratory, Richland, Washington.

Ryan, K., Mason, J.B., Evans, B., Vora, V., & Olson, A. (2008). Steam Reforming Technology Demonstration for Conversion of DOE Sodium-Bearing Tank Waste at Idaho National Laboratory into a Leach-Resistant Alkali Aluminosilicate Waste Form. *Proceedings of Waste Management 2008*, Phoenix, Arizona, February 2008

Schreiber, H.D. (2007). Redox of Model Fluidized Bed Steam Reforming Systems Final Report Report Subcontract AC59529T, VMI Research Laboratories, Lexington, Virginia.

Singh, D., Wagh, A.S., Cunnane, J.C., & Mayberry, J.L. (1997). Chemically Bonded Phosphate Ceramics for Low-Level Mixed-Waste Stabilization. *Journal of Environmental Science and Health Part A-Environmental Science and Engineering & Toxic and Hazardous Substance Control,* Vol. 32, No. 2, pp. 527-541

Singh, D., Wagh, A.S., Tlustochowicz, M., & Jeong, S.Y. (1998). Phosphate Ceramic Process for Macroencapsulation and Stabilization of Low-Level Debris Wastes. *Waste Management,* Vol. 18, No. 2, pp. 135-143

Soelberg, N.R., Marshall, D.W., Bates, S.O., & Taylor, D.D. (2004a). Phase 2 THOR® Steam Reforming Tests for Sodium-Bearing Waste Treatment. *INEEL*/EXT-04-01493, Idaho National Engineering and Environmental Laboratory, Idaho Falls, Idaho.

Soelberg, N.R., Marshall, D.W., Bates, S.O., & Siemer, D.D. (2004b) SRS Tank 48H Steam Reforming Proof-of-Concept Test Report, *INEEL/EXT-03-01118*, *Rev 1*, Idaho National Engineering and Environmental Laboratory, Idaho Falls, Idaho.

Spence, R.D., & Shi, C. (2005). *Stabilization and Solidification of Radioactive and Mixed Waste*. CRC Press, ISBN: 9781566704441, Boca Raton, Florida

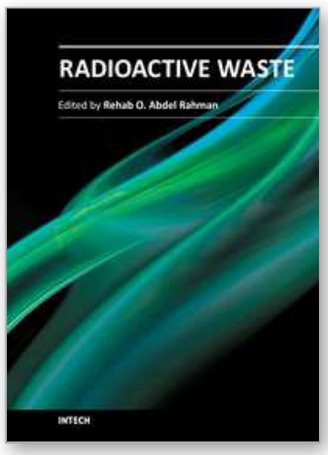
TTT. (2009). Report for Treating Hanford LAW and WTP SW Simulants: Pilot Plant Mineralizing Flowsheet. *RT-21-002*, THOR Treatment Technologies, LLC, Denver, Colorado.

Vora, V., Olson, A., Mason, B., Evans, B., & Ryan, K. (2009). Steam Reforming Technology Demonstration for Conversion of Hanford LAW Tank Waste and LAW Recycle Waste into a Leach Resistant Alkali Aluminosilicate Waste Form. *Proceedings of Waste Management 2009*, Phoenix, Arizona, March 2009

Wagh, A.S., Strain, R. Jeong, S.Y., Reed, D., Krause, T., & Singh, D. (1997). Stabilization of Rocky Flats Pu-Contaminated Ash within Chemically Bonded Phosphate Ceramics. *Journal of Nuclear Materials,* Vol. 265, No. 3, pp. 295-307

Wagh, A.S., Jeong, S.Y., & Singh, D. (1997). High Strength Phosphate Cement Using Industrial Byproduct Ashes. In: *Proceedings of First International Conference*, ed. A. Azizinamini et al., American Society of Civil Engineers. pp. 542-553

Williams, M.R., Jantzen, C.M., Burket, P.R., Crawford, C.L., Daniel, W.E., Aponte, C., & Johnson, C. (2010). 2009 Pilot Scale Fluidized Bed Steam Reforming Testing Using the THOR® (THermal Organic Reduction) Process: Analytical Results for Tank 48H Organic Destruction. *Proceedings of Waste Management 2010*, Phoenix, Arizona, October 2010




**Radioactive Waste**

Edited by Dr. Rehab Abdel Rahman

ISBN 978-953-51-0551-0
Hard cover, 502 pages
**Publisher** InTech
**Published online** 25, April, 2012
**Published in print edition** April, 2012

The safe management of nuclear and radioactive wastes is a subject that has recently received considerable recognition due to the huge volume of accumulative wastes and the increased public awareness of the hazards of these wastes. This book aims to cover the practice and research efforts that are currently conducted to deal with the technical difficulties in different radioactive waste management activities and to introduce to the non-technical factors that can affect the management practice. The collective contribution of esteem international experts has covered the science and technology of different management activities. The authors have introduced to the management system, illustrate how old management practices and radioactive accident can affect the environment and summarize the knowledge gained from current management practice and results of research efforts for using some innovative technologies in both pre-disposal and disposal activities.

**How to reference**

In order to correctly reference this scholarly work, feel free to copy and paste the following:

James J. Neeway, Nikolla P. Qafoku, Joseph H. Westsik Jr., Christopher F. Brown, Carol M. Jantzen and Eric M. Pierce (2012). Radionuclide and Contaminant Immobilization in the Fluidized Bed Steam Reforming Waste Product, Radioactive Waste, Dr. Rehab Abdel Rahman (Ed.), ISBN: 978-953-51-0551-0, InTech, Available from: http://www.intechopen.com/books/radioactive-waste/radionuclide-and-contaminant-immobilization-in-the-fluidized-bed-steam-reforming-waste-products

INTECH
open science | open minds

**InTech Europe**
University Campus STeP Ri
Slavka Krautzeka 83/A
51000 Rijeka, Croatia
Phone: +385 (51) 770 447
Fax: +385 (51) 686 166
www.intechopen.com

**InTech China**
Unit 405, Office Block, Hotel Equatorial Shanghai
No.65, Yan An Road (West), Shanghai, 200040, China
中国上海市延安西路65号上海国际贵都大饭店办公楼405单元
Phone: +86-21-62489820
Fax: +86-21-62489821

© 2012 The Author(s). Licensee IntechOpen. This is an open access article distributed under the terms of the Creative Commons Attribution 3.0 License, which permits unrestricted use, distribution, and reproduction in any medium, provided the original work is properly cited.

IntechOpen

IntechOpen